

# Delta Baryon Magnetic Moments From Lattice QCD

I.C. Cloet\*, D.B. Leinweber† and A.W. Thomas‡

*Special Research Centre for the Subatomic Structure of Matter and  
Department of Physics and Mathematical Physics, University of Adelaide, SA 5005, Australia*

Theoretical predictions for the magnetic moments of the physical  $\Delta$  baryons are extracted from lattice QCD calculations. We utilize finite-range regulated effective field theory that is constructed to have the correct Dirac moment mass dependence in the region where the  $u$  and  $d$  quark masses are heavy. Of particular interest is the chiral nonanalytic behaviour encountered as the  $N\pi$  decay channel opens. We find a  $\Delta^{++}$  magnetic moment (at the  $\Delta$  pole) of  $\mu_{\Delta^{++}} = 4.99 \pm 0.56 \mu_N$ . This result is within the Particle Data Group range of  $3.7\text{--}7.5 \mu_N$  and compares well with the experimental result of Bosshard *et al.* of  $\mu_{\Delta^{++}} = 4.52 \pm 0.51 \pm 0.45 \mu_N$ . The interplay between the different pion-loop contributions to the  $\Delta^+$  magnetic moment leads to the surprising result that the proton moment may exceed that of the  $\Delta^+$ , contrary to conventional expectations.

PACS numbers: 12.39.Fe, 12.38.Gc, 13.40.Em, 14.20.Gk

## I. INTRODUCTION

The magnetic moments of the  $\Delta$  baryons have already caught the attention of the experimental community and hold the promise of being accurately measured in the foreseeable future. Experimental estimates exist for the  $\Delta^{++}$ , based on the reaction  $\pi^+ p \rightarrow \pi^+ \gamma' p$ . The Particle Data Group [1] cites a range of values,  $3.7\text{--}7.5 \mu_N$ , for the  $\Delta^{++}$  magnetic moment, with the two most recent experimental results being  $\mu_{\Delta^{++}} = 4.52 \pm 0.51 \pm 0.45 \mu_N$  [2] and  $\mu_{\Delta^{++}} = 6.14 \pm 0.51 \mu_N$  [3]. This gives an idea of the elusive nature of the  $\Delta$  magnetic moments. In principle, the  $\Delta^+$  magnetic moment can be obtained from the reaction  $\gamma p \rightarrow \pi^0 \gamma' p$ , as demonstrated at the Mainz microtron [4, 5] and Kotulla *et al.* have recently reported an initial measurement of  $\mu_{\Delta^+} = 2.7^{+1.0}_{-1.3}(\text{stat.}) \pm 1.5(\text{syst.}) \pm 3(\text{theor.}) \mu_N$  [6].

Recent extrapolations of octet baryon magnetic moments have utilized a Padé approximant [7, 8, 9, 10], an analytic continuation of chiral perturbation theory ( $\chi$ PT) which incorporates the correct leading nonanalytic (LNA) structure of  $\chi$ PT. This idea was recently extended to a study of decuplet baryons in the Access Quark Model [11], where the next-to-leading nonanalytic (NLNA) structure of  $\chi$ PT was also included. Incorporating the NLNA terms into the extrapolation function contributes little to the octet baryon magnetic moments, however it proves vital for the decuplet. This is because the NLNA terms from  $\chi$ PT contain information regarding the branch point at the octet-decuplet mass-splitting,  $m_\pi = \delta$ , associated with the  $\Delta \rightarrow N\pi$  decay channel, which plays a significant role in decuplet magnetic moments. Here we include the NLNA behaviour in a chiral extrapolation of the magnetic moments of the  $\Delta$  baryons

calculated in lattice QCD.

Although the Padé technique provides a well behaved method of extending  $\chi$ PT to heavy quark masses, it is not so obvious how it could be extended to higher order in a chiral expansion. We have therefore chosen to calculate explicitly the pion loop diagrams which give rise to the LNA and the NLNA behaviour of the  $\Delta$  magnetic moments using finite-range regularization [12, 13]. In this investigation we select the dipole-vertex regulator. We stress that, in the context of the chiral extrapolation of lattice QCD data, the use of a finite-range regulator is the preferred alternative to dimensional regularization as demonstrated in Ref. [12]. Ideally, the regulator mass should be constrained by lattice QCD results. However, the data available lies at large quark masses and provides little guidance. As such, we explicitly explore the regulator-mass dependence of our results, finding a sensitivity of 3.6% or less in the charged  $\Delta$  magnetic moments, for variation of the dipole mass parameter in the range 0.5–1.0 GeV.

## II. EXTRAPOLATIONS – AN EFFECTIVE FIELD THEORY

To one-loop order the dimensionally-regulated  $\chi$ PT result for decuplet baryon magnetic moments is [14, 15]

$$\mu_i = a_0 + \sum_{j=\pi, K} \frac{M_N}{32\pi^2 f_j^2} \left( \alpha_j^i \frac{4}{9} \mathcal{H}^2 \mathcal{F}(0, m_j, \mu) + \beta_j^i \mathcal{C}^2 \mathcal{F}(-\delta, m_j, \mu) \right) + a_2 m_\pi^2. \quad (1)$$

The  $\mathcal{F}(\delta, m_j, \mu)$  functions (with  $\delta$  the octet-decuplet mass difference) are the nonanalytic components of the meson loop diagrams shown in Fig. 1. These expressions are given explicitly in Ref. [14]. The constants  $a_0$  and  $a_2$  multiplying the analytic terms are not specified within  $\chi$ PT and must be determined by other means.

\*icloet@physics.adelaide.edu.au

†dleinweb@physics.adelaide.edu.au

‡athomas@physics.adelaide.edu.au

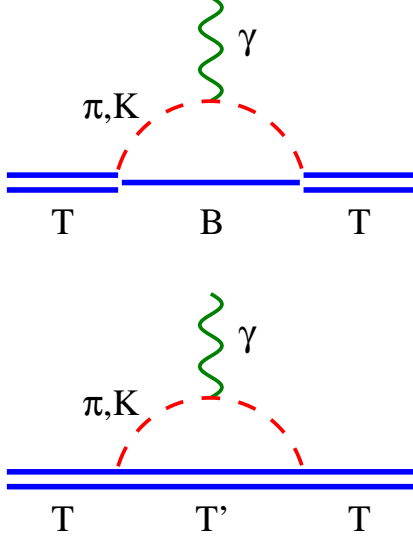


FIG. 1: Diagrams indicating the leading and next-to-leading contributions included in the calculations. The letters T and B correspond to decuplet and octet baryons respectively. The dashed line is the appropriate meson accompanying the baryon transition. The analytic expressions for these diagrams are given explicitly in Eqs. (3).

It is well known that dimensionally-regulated  $\chi$ PT expansions for baryon properties are troubled by a lack of clear convergence [16, 17, 18, 19]. This problem must be addressed if  $\chi$ PT results are to be applied far beyond the chiral limit, for example in the extrapolation of lattice data where pion masses up to 1 GeV are involved. Indeed, truncated dimensionally-regulated  $\chi$ PT expansions for magnetic moments exhibit the incorrect behaviour for large  $m_\pi$ . To address these concerns we adopt finite-range regulated  $\chi$ PT by calculating the meson-loop diagrams using a dipole-vertex regulator. The loop contributions then approach zero naturally as  $m_\pi$  becomes large. We combine the analytic terms of the chiral expansion into a single term that maintains the chiral expansion to the order we are working, while guaranteeing the correct magnetic moment mass dependence at heavy pion masses.

The extrapolation function which we employ to obtain decuplet baryon magnetic moment predictions from lattice QCD data, thus takes the form

$$\mu = \frac{a_0}{1 + c_0 m_\pi^2} + \sum_{T'} \chi_{T'}^j G_{TT'}(m_j, \Lambda) + \sum_B \chi_B^j G_{TB}(m_j, \delta, \Lambda), \quad (2)$$

where the sums over  $T'$  and  $B$  include the decuplet and octet intermediate states, respectively. The first term encapsulates the pion mass dependence of the photon field

| $\Delta^{++}$ |        | $\Delta^+$    |        | $\Delta^0$    |        | $\Delta^-$ |        |
|---------------|--------|---------------|--------|---------------|--------|------------|--------|
| Channel       | $\chi$ | Channel       | $\chi$ | Channel       | $\chi$ | Channel    | $\chi$ |
| $\Delta^+$    | 0.265  | $\Delta^0$    | 0.353  | $\Delta^-$    | 0.265  | $\Delta^0$ | -0.265 |
| $\Sigma^{*+}$ | 0.184  | $\Delta^{++}$ | -0.265 | $\Delta^+$    | -0.353 | $n$        | -0.795 |
| $p$           | 0.795  | $\Sigma^{*0}$ | 0.123  | $\Sigma^{*-}$ | 0.061  |            |        |
| $\Sigma^+$    | 0.552  | $n$           | 0.265  | $p$           | -0.265 |            |        |
|               |        | $\Sigma^0$    | 0.368  | $\Sigma^-$    | 0.184  |            |        |

TABLE I: The chiral coefficients for each intermediate state for  $\Delta$  baryon transitions.

coupling directly to the baryon and reflects previous success in the extrapolation of octet baryon magnetic moments [7, 8, 10]. This term ensures the correct behaviour, as a function of quark mass, of the Dirac moments of the quarks at heavy quark masses (as  $m_\pi^2 \propto m_q$  up to 1 GeV<sup>2</sup> – above this range one should use  $m_q$  directly). The parameters  $a_0$  and  $c_0$  are chosen to optimize the fit to lattice data. The functions  $G_{TT'}(m_j, \Lambda)$  and  $G_{TB}(m_j, \delta, \Lambda)$  are the (heavy baryon) loop contributions to the magnetic form factors, in the limit  $q \rightarrow 0$ , for decuplet-decuplet and decuplet-octet transitions respectively, see Fig. 1. These functions are given by

$$G_{TT'}(m_j, \Lambda) = \lim_{q \rightarrow 0} \frac{1}{2\pi} \int d^3k \mathcal{U}(k) \mathcal{U}(k') \frac{(\hat{q} \times \vec{k})^2}{(\omega_k \omega_{k'})^2},$$

$$G_{TB}(m_j, \delta, \Lambda) = \lim_{q \rightarrow 0} \frac{1}{2\pi} \int d^3k \mathcal{U}(k) \mathcal{U}(k') \frac{(\omega_k + \omega_{k'} - \delta)(\hat{q} \times \vec{k})^2}{\omega_k \omega_{k'} (\omega_k + \omega_{k'}) (\omega_k - \delta) (\omega_{k'} - \delta)}, \quad (3)$$

where  $q$ ,  $k$ ,  $k'$  are the momenta of the photon, incoming meson and outgoing meson, respectively. Note,  $\vec{k}' = \vec{k} + \vec{q}$  and  $\omega_k = \sqrt{k^2 + m_j^2}$ . The functions  $\mathcal{U}(k)$  and  $\mathcal{U}(k')$  are used to regulate the loop integrals - we use a dipole with a finite mass parameter  $\Lambda$ . Therefore

$$\mathcal{U}(k) = \left( \frac{\Lambda^2}{\Lambda^2 + k^2} \right)^2, \quad (4)$$

$$\mathcal{U}(k') = \left( \frac{\Lambda^2}{\Lambda^2 + (k')^2} \right)^2. \quad (5)$$

The masses,  $m_j$ , of Eq. (2) are octet-meson masses associated with the meson cloud and  $\chi_i$  are model independent constants [20] that give the magnitude of the loop contribution for each intermediate baryon state. These coefficients are given by [14]

$$\chi_{T_i}^{(\pi)} = \frac{M_N \mathcal{H}^2}{72 \pi^2 (f_\pi)^2} \alpha_{T_i}^{(\pi)}, \quad \chi_{T_i}^{(K)} = \frac{M_N \mathcal{H}^2}{72 \pi^2 (f_K)^2} \alpha_{T_i}^{(K)},$$

$$\chi_{B_i}^{(\pi)} = \frac{M_N \mathcal{C}^2}{32 \pi^2 (f_\pi)^2} \beta_{B_i}^{(\pi)}, \quad \chi_{B_i}^{(K)} = \frac{M_N \mathcal{C}^2}{32 \pi^2 (f_K)^2} \beta_{B_i}^{(K)}, \quad (6)$$

where  $\mathcal{H}$  describes meson couplings to decuplet baryons and  $\mathcal{C}$  is the octet-decuplet coupling constant. We assign  $\mathcal{H}$  and  $\mathcal{C}$  their  $SU(6)$  values of  $\mathcal{H} = -3D$  and  $\mathcal{C} = -2D$  [21] where the tree level value for  $D$  is 0.76. The decay constants take the values  $f_\pi = 93$  MeV and  $f_K = 1.2 f_\pi$  [22], appropriate to an expansion about the chiral  $SU(2)$  limit. Note also that  $M_N$  is the nucleon mass and the parameters  $\alpha$  and  $\beta$  are given in Ref. [23]. The model independent loop coefficients,  $\chi$ , are summarized in Table I.

In these calculations the complex mass scheme [3, 24] is adopted as a method of incorporating the finite life of the  $\Delta$  resonances, whilst also retaining electromagnetic gauge invariance. That is, one aims to extract the magnetic moment of the  $\Delta$  at the pole position in the complex energy plane,  $\delta^{(\text{pole})} \equiv \delta_R - i\delta_I = 270 - i50$  MeV [1] for the physical pion mass ( $m_\pi^{\text{phys}}$ ). Since the value at the position of the  $\Delta$  pole is independent of the path chosen, we illustrate extrapolations along the path  $\delta_R$  constant and  $\delta_I$  given by

$$\delta_I = G \pi (\delta_R^2 - m_\pi^2)^{\frac{3}{2}} \left( \frac{\Lambda^2}{\Lambda^2 + \delta_R^2 - m_\pi^2} \right)^4 \Theta(\delta_R - m_\pi). \quad (7)$$

The latter is motivated by the usual expression for the  $\Delta \rightarrow N \pi$  self-energy [12], with  $G$  chosen to ensure  $\delta_I = 50$  MeV at  $m_\pi^{\text{phys}}$ .

To relate the kaon and pion masses we utilize the following relations provided by  $\chi$ PT

$$m_K^2 = m_K^{(0)2} + \frac{1}{2} m_\pi^2, \quad (8)$$

$$m_K^{(0)} = \sqrt{(m_K^{\text{phys}})^2 - \frac{1}{2}(m_\pi^{\text{phys}})^2}. \quad (9)$$

This allows us to also incorporate kaon loops (at fixed strange quark mass) in extrapolations as a function of  $m_\pi^2$ , to the physical mass regime.

If we expand the first term of Eq. (2) as a Taylor series about  $m_\pi = 0$  to order  $\mathcal{O}(m_\pi^4)$ , and take the limit as  $\Lambda \rightarrow \infty$  in the loop integrals, we obtain the traditional  $\chi$ PT expansion for decuplet magnetic moments, as given in Eq. (1) (where the infinite constants encountered in dimensional regularization simply redefine  $a_0$ ). Further, since the loop contributions approach zero much faster than  $1/m_\pi^2$  for any reasonable value of  $\Lambda$ , Eq. (2) guarantees the correct mass dependence of the Dirac magnetic moment in the heavy quark mass regime. From previous studies of the nucleon axial form factor [25] it has been consistently demonstrated that  $\Lambda$  in the dipole regulator must have a magnitude  $< 1$  GeV. For this investigation we assign  $\Lambda = 0.8$  GeV, the optimal value obtained in analyses of state of the art full QCD simulations of the nucleon mass [12].

In Fig. 2 we plot Eqs. (3) (without the chiral coefficient prefactors) with the above value of  $\delta$  and a regulator of  $\Lambda = 0.8$  GeV. Four types of intermediate baryon states are considered. The opening of the  $N \pi$  decay channel has

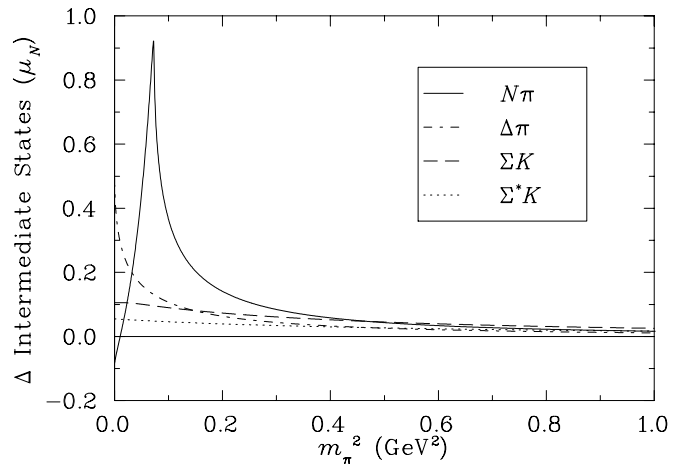


FIG. 2: Plots of the four types of loop contributions to the  $\Delta$  magnetic moments (without the coefficients) that are considered here. These plots are obtained from Eqs. (3), where we have used the complex mass scheme as a gauge invariant method with which to incorporate the finite life-time of the  $\Delta$  resonances.

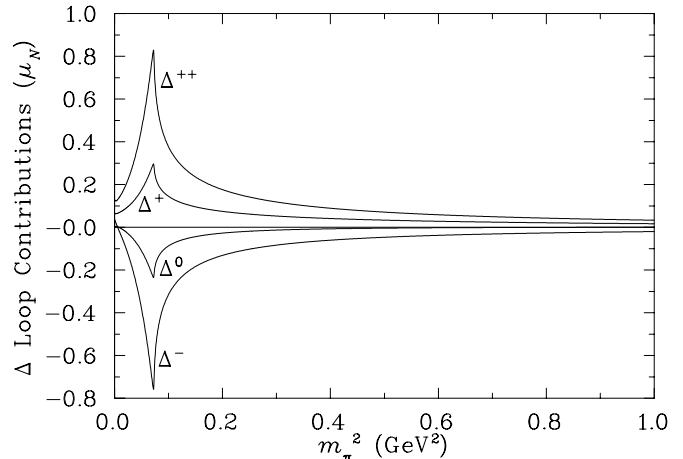


FIG. 3: Plots of the total loop contribution considered for each  $\Delta$  baryon. These curves are the sum of the functions plotted in Fig. 2 multiplied by the appropriate coefficients listed in Table I.

an interesting effect on the magnetic moment contribution. Fig. 3 presents a plot of the total loop contribution for each  $\Delta$  baryon, determined using Eqs. (3) and the chiral coefficients given in Table I.

### III. RESULTS

The lattice QCD results given in Table II are extracted from Ref. [26]. These lattice calculations employ sequential-source three-point function based techniques [27] utilizing the conserved vector current such that no renormalization is required in relating the lattice results

| kappa | Baryon Mass<br>(GeV) | Pion Mass<br>(GeV) | $\Delta^{++}$<br>( $\mu_N$ ) | $\Delta^+$<br>( $\mu_N$ ) | $\Delta^-$<br>( $\mu_N$ ) | $\Delta^0$<br>( $\mu_N$ ) |
|-------|----------------------|--------------------|------------------------------|---------------------------|---------------------------|---------------------------|
| 0.152 | 1.74 (50)            | 0.964 (12)         | 2.81 (18)                    | 1.40 (9)                  | 0.000 (00)                | -1.40 (9)                 |
| 0.154 | 1.57 (60)            | 0.820 (11)         | 3.19 (28)                    | 1.59 (14)                 | 0.000 (00)                | -1.59 (14)                |
| 0.156 | 1.39 (80)            | 0.665 (13)         | 3.67 (43)                    | 1.83 (21)                 | 0.000 (00)                | -1.83 (21)                |

TABLE II: Quenched lattice QCD magnetic moments for the  $\Delta$  baryons extracted from Ref. [26]. Uncertainties are obtained using a third-order single-elimination jack-knife error analysis. Lattice results for the  $\Delta^0$  are exactly zero, in the quenched approximation.

to the continuum. These simulations utilized twenty-eight quenched gauge configurations on a  $24 \times 12 \times 12 \times 24$  periodic lattice at  $\beta = 5.9$ , corresponding to a lattice spacing of 0.128(10) fm. Moments are obtained from the form factors at 0.16 GeV<sup>2</sup> by assuming equivalent  $q^2$  dependence for both the electric and magnetic form factors. This assumption will be tested in future studies incorporating the ideas presented here. Uncertainties are statistical in origin and are estimated by a third-order single-elimination jack-knife analysis [28].

In Figs. 4–7 we present fits of the extrapolation function, Eq. (2), to the lattice data as a function of  $m_\pi^2$ . The resulting magnetic moment predictions, along with the fit parameters  $a_0$  and  $c_0$ , are summarized in Table III. In Fig. 4 we show two experimental values for the  $\Delta^{++}$  magnetic moment, the result  $\mu_{\Delta^{++}} = 4.52 \pm 0.50 \pm 0.45 \mu_N$  is from Ref. [2] and  $\mu_{\Delta^{++}} = 6.14 \pm 0.51 \mu_N$  is given in Ref. [3]. The discrepancy between these two results is a reasonable indication of the current level of systematic error in the experimental determination of the  $\Delta^{++}$  magnetic moment. Our prediction of  $\mu_{\Delta^{++}} = 4.99 \pm 0.56 \mu_N$  agrees well with the first experimental result, however it lies slightly below the range of the second. We note that the approach used in Ref. [3] does not respect unitarity and when this shortcoming is addressed the authors find  $\mu_{\Delta^{++}} = 6.01 \pm 0.61 \mu_N$  [3], resulting in a somewhat better agreement between our prediction and this experimental result. The result reported here for the  $\Delta^+$  magnetic moment of  $2.49 \pm 0.27 \mu_N$  is in agreement with the initial measurement of Kotulla *et al.* [6], namely  $\mu_{\Delta^+} = 2.7^{+1.0}_{-1.3}(\text{stat.}) \pm 1.5(\text{syst.}) \pm 3(\text{theor.})\mu_N$ , however the experimental error at this time is still very large.

To address the issue of regulator-mass dependence we vary  $\Lambda$  between 0.5 and 1.0 GeV, in each case readjusting  $a_0$  and  $c_0$  to fit the lattice data and find only a slight regulator-mass dependence of 3.6% or less, for each of the charged  $\Delta$  baryons. Ultimately, lattice results at lighter quark masses will constrain  $\Lambda$  and therefore reduce this uncertainty.

The inclusion of the  $\Delta^0$  is more for completeness rather than a firm result, as the lattice data in quenched QCD yields identically zero in this case. By varying the regulator  $\Lambda$  between 0.5 and 1.0 GeV we find the moment remains positive, with the order of magnitude of our result unchanged. We await new, unquenched lattice data in order to obtain a stronger prediction for the  $\Delta^0$  mag-

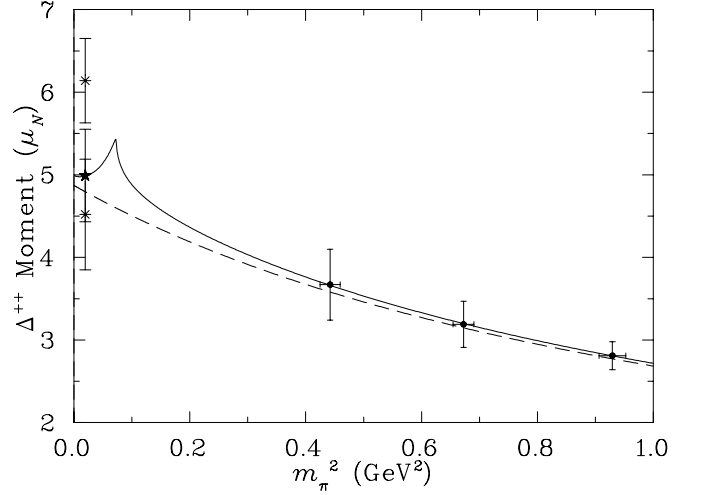


FIG. 4: The fit (solid line) to the lattice QCD data (solid circles) for the  $\Delta^{++}$  magnetic moment using the extrapolation function, Eq. (2). The dashed line is the plot of the first term of Eq. (2) - and reflects the analytic terms of the chiral expansion. The solid star (\*) indicates the prediction of the extrapolated lattice data. The two most recent experimental results are indicated by the two asterisks (\*), where the smaller prediction is taken from Ref. [2] and the larger from Ref. [3].

netic moment.

The interesting feature of the plots given in Figs. 4–7 is the cusp at  $m_\pi = \delta$  which indicates the opening of the octet decay channel,  $\Delta \rightarrow N\pi$ . The physics behind the cusp is intuitively revealed by the relation between the derivative with respect to  $m_\pi^2$  of the magnetic moment and the derivative with respect to the momentum transfer,  $q^2$ , provided by the pion propagator  $1/(q^2 + m_\pi^2)$  in the heavy baryon limit. Derivatives with respect to  $q^2$  are proportional to the magnetic radius in the limit  $q^2 \rightarrow 0$

$$\langle r_M^2 \rangle = -6 \frac{dG_M(q^2)}{dq^2} \Big|_{q^2=0}. \quad (10)$$

If we consider for example  $\Delta^{++} \rightarrow p\pi^+$ , with  $|j, m_j\rangle = |3/2, 3/2\rangle$ , the  $N\pi$  state is in relative P-wave orbital angular momentum with  $|l, m_l\rangle = |1, 1\rangle$ . Thus the pion makes a positive contribution to the magnetic moment.

| Baryon        | $a_0$ | $c_0$ | Lattice ( $\mu_N$ ) | Experiment ( $\mu_N$ )   |
|---------------|-------|-------|---------------------|--|
| $\Delta^{++}$ | 4.87  | 0.82  | 4.99 (56)           | 3.7–7.5  |
| $\Delta^+$    | 2.44  | 0.83  | 2.49 (27)           | $2.7^{+1.0}_{-1.3}(\text{stat.}) \pm 1.5(\text{syst.}) \pm 3(\text{theor.})$ |
| $\Delta^0$    | 0.63  | 381   | 0.06 (00)           |  |
| $\Delta^-$    | -2.40 | 0.80  | -2.45 (27)          |  |

TABLE III: Theoretical predictions for the four  $\Delta$  baryon magnetic moments from extrapolated lattice QCD results. The quoted errors are statistical in origin. The fit parameters  $a_0$  and  $c_0$  are given for each scenario. The experimental values for the  $\Delta^{++}$  and  $\Delta^+$  magnetic moments are taken from Ref. [1]. and Ref. [6], respectively.

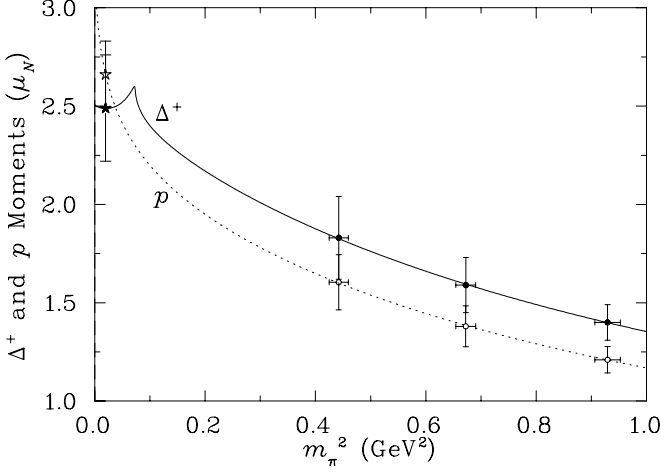


FIG. 5: The fit (solid line) to the lattice QCD data (solid circles) for the  $\Delta^+$  magnetic moment using the extrapolation function, Eq. (2). The theoretical prediction for the  $\Delta^+$  magnetic moment is indicated by a solid star (\*). The initial experimental value for the  $\Delta^+$  magnetic moment is discussed in the text. The proton extrapolation (dotted line) of the lattice QCD simulation results of Ref. [29] (open circles) is included for reference.

As the opening of the  $p\pi^+$  decay channel is approached from the heavy quark-mass regime, the range of the pion cloud increases. Just above threshold the pion cloud extends towards infinity as  $\Delta E \rightarrow 0$ ,  $\Delta E \Delta t \sim \hbar$  and the radius of the magnetic form factor diverges similarly,  $(\partial/\partial q^2)G_M \propto (\partial/\partial m_\pi^2)G_M \rightarrow -\infty$  from above threshold. Below threshold,  $G_M$  becomes complex and the magnetic moment of the  $\Delta$  is identified with the real part. The imaginary part describes the physics associated with photon-pion coupling in which the pion is subsequently observed as a decay product. Therefore decuplet to octet transitions enhance the  $\Delta$  magnetic moments when the octet decay channel is closed. However, as the decay channel opens this physics serves to suppress the magnetic moment as the chiral limit is approached. These transitions are energetically favourable, making them of paramount importance in determining the physical properties of  $\Delta$  baryons.

The inclusion of octet–decuplet transitions in octet magnetic moment extrapolations is less important. Sig-

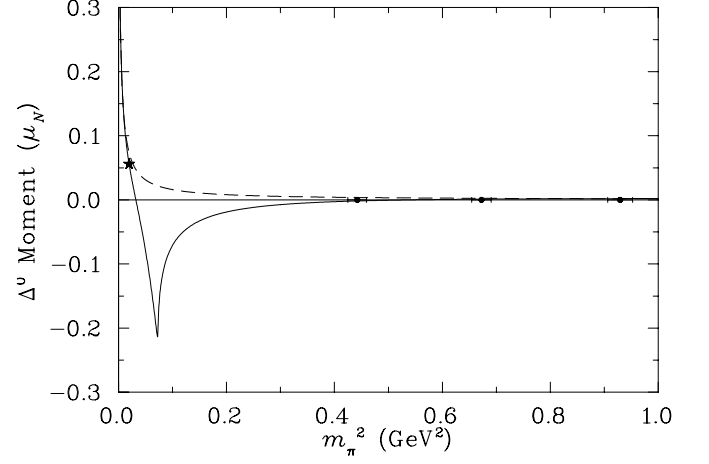


FIG. 6: The fit to the lattice QCD data for the magnetic moment of the  $\Delta^0$ , using the extrapolation function, Eq. (2). Symbols are as in Fig. 4. There is currently no experimental value for the  $\Delta^0$  magnetic moment.

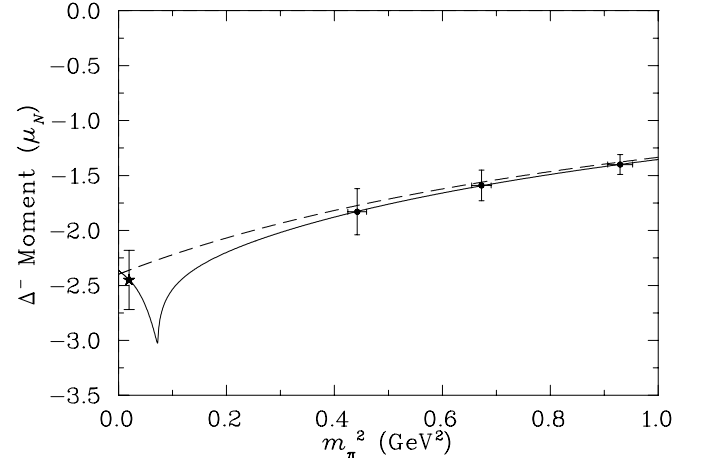


FIG. 7: The fit to the lattice QCD data for the magnetic moment of the  $\Delta^-$ , using the extrapolation function, Eq. (2). Symbols are as in Fig. 4. There is currently no experimental value for the  $\Delta^-$  magnetic moment.

nificant energy must be borrowed from the vacuum for these transitions to occur. The formulation of effective field theory with a finite-range regulator naturally suppresses transitions from ground state octet baryons to excited state baryons. Physically, the finite size of the meson-cloud source suppresses these high energy contributions. Hence any new curvature associated with octet-decuplet transitions for octet baryons is small [7]. Indeed, the inclusion of the  $p \rightarrow \Delta \pi$  channels in the proton moment extrapolation of Fig. 5 increases the predicted moment by only  $0.05 \mu_N$  from  $2.61$  to  $2.66 \mu_N$ . For this reason octet to decuplet transitions have been omitted in other chiral extrapolation studies of the octet magnetic moments [8, 10].

In the simplest SU(6) quark model with  $m_u = m_d$  the  $\Delta^+$  and proton moments are equal. However most quark models include spin dependent  $q-q$  interactions that enhance the  $\Delta^+$  magnetic moment relative to the proton. This phenomenology is supported by the lattice results [26] at large quark masses. Consequently, previous linearly extrapolated lattice predictions [26], using the same lattice data, suggested that the  $\Delta^+$  moment should be greater than that of the proton. We find evidence that supports a different conclusion, with predicted values for the  $\Delta^+$  and proton moments lying close at  $2.49(27) \mu_N$  and  $2.66(17) \mu_N$ , respectively. The primary reason for this result is the interplay between the three different pion loop contributions;  $\Delta^+ \rightarrow \Delta^{++} \pi^-$ ,  $n \pi^+$  and  $\Delta^0 \pi^+$ . The transition to a  $\Delta^{++} \pi^-$  state largely cancels the  $n \pi^+$  contribution, which dominates the proton magnetic moment. This means that the  $\Delta^0 \pi^+$  transition is the main loop contribution to the  $\Delta^+$  magnetic moment, where the  $\Delta^+ \rightarrow \Delta^0 \pi^+$  coupling is weak, relative to that of the  $p \rightarrow n \pi^+$  transition.

The proton magnetic moment extrapolation is included in Fig. 5, and provides an illustration of the importance of incorporating known chiral physics in any extrapolation to the physical world. Thus, an experimental value for the  $\Delta^+$  magnetic moment would offer very important insight into the role of spin dependent forces and

chiral nonanalytic behaviour in the structure of baryon resonances.

#### IV. CONCLUSION

Finite-range regulated  $\chi$ PT has been applied to the extrapolation of lattice QCD results for the decuplet baryon magnetic moments. The magnetic moments of the four  $\Delta$  baryons at the resonance pole are determined. Experimental values exist only for the  $\Delta^{++}$  magnetic moment. A result for the  $\Delta^+$  should be forthcoming in the near future. The Particle Data Group gives a range of  $3.7-7.5 \mu_N$  for the  $\Delta^{++}$  moment, with the two most recent experimental results being  $\mu_{\Delta^{++}} = 4.52 \pm 0.51 \pm 0.45 \mu_N$  [2] and  $\mu_{\Delta^{++}} = 6.14 \pm 0.51 \mu_N$  [3]. Our lattice QCD prediction of  $\mu_{\Delta^{++}} = 4.99 \pm 0.56 \mu_N$  compares well with the first of these experimental results. An interesting result from this investigation is the prediction that the  $\Delta^+$  magnetic moment lies close to and probably below that of the proton moment. Therefore a new high precision experimental measurement of the  $\Delta^+$  moment would offer valuable insight into spin dependent forces and chiral nonanalytic behaviour of excited states. The lattice data used in these calculations is now over 10 years old, determined with pion masses greater than 600 MeV. The arrival of new lattice data at lower pion masses is therefore eagerly anticipated, and will help constrain the fit parameters and associated statistical uncertainties. All of this should be forthcoming in the next few years and offers an excellent opportunity to test the predictions of QCD.

#### Acknowledgments

We thank Ross Young for interesting and helpful discussions. This work was supported by the Australian Research Council and the University of Adelaide.

- 
- [1] K. Hagiwara *et al.* [Particle Data Group Collaboration], Phys. Rev. D **66**, 010001 (2002).
  - [2] A. Bosshard *et al.*, Phys. Rev. D **44**, 1962 (1991).
  - [3] G. Lopez Castro and A. Mariano, Nucl. Phys. A **697**, 440 (2002).
  - [4] M. Kotulla [TAPS and A2 Collaborations], *Prepared for Hirscheegg '01: Structure of Hadrons: 29th International Workshop on Gross Properties of Nuclei and Nuclear Excitations, Hirscheegg, Austria, 14-20 Jan 2001*.
  - [5] D. Drechsel and M. Vanderhaeghen, Phys. Rev. C **64**, 065202 (2001).
  - [6] M. Kotulla *et al.*, Phys. Rev. Lett. **89**, 272001 (2002).
  - [7] D. B. Leinweber, D. H. Lu and A. W. Thomas, Phys. Rev. D **60**, 034014 (1999).
  - [8] E. J. Hackett-Jones, D. B. Leinweber and A. W. Thomas, Phys. Lett. B **489**, 143 (2000).
  - [9] D. B. Leinweber, A. W. Thomas and R. D. Young, Phys. Rev. Lett. **86**, 5011 (2001).
  - [10] I. C. Cloet, D. B. Leinweber and A. W. Thomas, Phys. Rev. C **65**, 062201 (2002).
  - [11] I. C. Cloet, D. B. Leinweber and A. W. Thomas, in Proc. of the Joint Workshop on "Physics at Japanese Hadron Facility", eds. V. Guzey *et al.*, 125-135, World Scientific (2002), arXiv:nucl-th/0211027.
  - [12] R. D. Young, D. B. Leinweber and A. W. Thomas, *To appear in: Progress in Particle and Nuclear Physics*, arXiv:hep-lat/0212031.
  - [13] J. F. Donoghue, B. R. Holstein and B. Borasoy, Phys. Rev. D **59**, 036002 (1999).
  - [14] M. K. Banerjee and J. Milana, Phys. Rev. D **54**, 5804 (1996).
  - [15] This definition of  $\mu_i$  corrects a sign error in Ref. [14].

There the  $\beta_j^i \dots$  term is preceded by a minus sign.

- [16] T. Hatsuda, Phys. Rev. Lett. **65**, 543 (1990).
- [17] S. V. Wright, Ph. D. thesis (The University of Adelaide, 2002).
- [18] C. Bernard, S. Hashimoto, D. B. Leinweber, P. Lepage, E. Pallante, S. R. Sharpe and H. Wittig, arXiv:hep-lat/0209086.
- [19] A. W. Thomas, “Chiral extrapolation of hadronic observables”, arXiv:hep-lat/0208023.
- [20] L. F. Li and H. Pagels, Phys. Rev. Lett. **26**, 1204 (1971).
- [21] M. N. Butler, M. J. Savage and R. P. Springer, Nucl. Phys. B **399**, 69 (1993).
- [22] E. Jenkins, M. E. Luke, A. V. Manohar and M. J. Savage, Phys. Lett. B **302**, 482 (1993) [Erratum-ibid. B **388**, 866 (1996)].
- [23] M. N. Butler, M. J. Savage and R. P. Springer, Phys. Rev. D **49**, 3459 (1994).
- [24] M. El Amiri, J. Pestieau and G. Lopez Castro, Nucl. Phys. A **543**, 673 (1992).
- [25] P. A. M. Guichon, G. A. Miller and A. W. Thomas, Phys. Lett. B **124**, 109 (1983).
- [26] D. B. Leinweber, T. Draper and R. M. Woloshyn, Phys. Rev. D **46**, 3067 (1992).
- [27] Magnetic Moment contributions from the coupling of the electromagnetic current directly to sea-quark loops are neglected in these simulations. However, the net effect from  $u$ ,  $d$  and  $s$  sea-quark loops is small due to approximate SU(3)-flavour symmetry where the net loop contribution vanishes.
- [28] B. Efron, SIAM Rev. **21**, 460 (1979).
- [29] D. B. Leinweber, R. M. Woloshyn and T. Draper, Phys. Rev. D **43**, 1659 (1991).